Significance of Multiple Slip Effects on Falkner-Skan Wedge Flow of Nanofluid with Nonlinear Thermal Radiation.

P. Mishra[1], M.R. Acharya[2*]

[1] Research Scholar, CBSH, O.U.A.T, Bhubaneswar-751003, Odisha, India

[2]Department of Physics, CBSH, O.U.A.T, Bhubaneswar-751003, Odisha, India*

Abstract

The liquid molecules slip at the solid surface for a length scale less than mean free path of the molecules. The slip boundary conditions are essential to study fluid flow in nanoscale level. Therefore it is proposed to study slip flow (both 1^{st} and 2^{nd} order) in velocity, temperature and concentration associated with a nanofluid past a wedge. The flow model consists of Brownian motion, thermophoresis multiple slips of higher order and non-linear thermal radiation. Transport equations are converted into third order ordinary differential equations and then solved by using Runge-Kutta method. The 1^{st} order slip parameter increases the velocity and second order slip parameter diminishes velocity. Local heat transfer coefficient drops due 1^{st} order and 2^{nd} order slip parameters. However 1^{st} order slip parameter enhances volume fraction and 2^{nd} order slip parameter diminishes the volume fraction. The effects of other parameters are calculated and depicted graphically.

Key Words: *Wedge flow, Nanofluid, Brownian motion, Multiple slips of higher order*

PACS NO. 05.40. Jc, 41.20Gz, 47.45. Gx, 44.40. +a

1. Introduction

During last few decades engineering and technology has contributed lot to the development of thermal science. This is perhaps due to characteristics features of nanofluid. In this context enhancement of thermal conductivity and heat transfer of nanofluid has been studied extensively. Thermal conductivity of nanofluid is greater than thermal conductivity of ordinary fluid was first presented by choi et al. [1]. Nanoparticle (<100 nm) in suspension of base fluid can be prepared in following methods (i) one step method (ii) two step method and (iii) new methods [2,3]. The advantages and disadvantages of all such methods are studied in great extent by Yu and Xie [4]. Models involving transport of nanofluids can be presented by using proposal of Buongiorno [5] or Tiwari and Das [6]. In this context Buongiorno's model with diffusion and thermophoresis are taken into account. This model consists of two component and four equations two demonstrate nanofluid transport. Particularly nanoparticles (Fe_2O_3, Al_2O_3, Al, Fe, Hg) in base fluid (H_2O, $C_2H_6O_2$) are used to make nanofluids. Several models [7,8,9,10] have been proposed to study single phase model to calculate physical properties relating to nanofluid flow. Sheikholeslami et al [11] have investigated diffusion of thermophoresis parameter with magnetic field on nanofluid flow. Semi-analytical and numerical approach [12] has been used to discuss convective heat transfer of nanofluid. A study on two phase nanofluid MHD flow has been proposed to study thermal radiation effect [13]. Ali et al [14] examined nanofluid flow over wedge using Buongiorno's model with the help of similarity solution. Temperature dependent heat source in association with MHD nanofluid flow over a wedge has been studied by Mishra et al. [15]. Importance of thermodynamic irreversibility together with activation energy over a non-isothermal wedge using Brownian diffusion has been investigated by Acharya et al. [16].

The mean velocity of fluid molecules cannot be equal to wall velocity for a distance less or equal to mean free path under no slip boundary condition. Actually, molecules slip at the solid wall for nanoscale system. Slip velocity is essential to predict flow pattern. Slip models (1st order, 2nd order etc.) are derived from kinetic theory and Fukut-Kaheko (F-K) model is the computational solution of linearized Boltzmann equation-K model based on flow configuration and not suitable for practical purpose. However, slip models tend to F-K model in the limit Kn<1 (Kn =λ/h) [17]. Where Kn denotes Knudsen number, λ denotes mean free path and h represents distance. So slip models in above limit are useful in technological processes. Slip models move away from linearized Boltzmann solution with reference to high Knudsen number. Lubrication of disk drive and flow inside a nano tube are few potential applications of slip velocity in nanofluid flow.

*Corresponding author, manasranjan_acharya@yahoo.co.in

Let us focus our attention to discuss wedge flow with slip boundary conditions. At the outset Martin and Boyd [18] studied wedge flow with velocity slip along with thermal jump. They noticed that rarefaction effect produces decrease in heat transfer. Nanofluid flow over stretching surface using slip condition in velocity, temperature and

concentration has been studied by Awais et al [19]. Liu et al [20] considered physical fluid properties and higher order slip condition in velocity together with temperature jump to study nanofluid flow over a wedge. They observed drop in velocity and temperature for higher order slip and jump condition. Pandey and Kumar [21] investigated wedge flow with slip and jump condition over a wedge in porous medium. They found reduction in thickness of thermal boundary layer due to slip parameter. A different mass flux condition with Carreau nanofluid over has been point of discussion [22]. In this case reduction in local Sherwood number is observed due to decrease in velocity slip parameter. Keller –Box scheme is applied to solve slip condition with MHD nanofluid flow over a stretching sheet [23]. They pointed out a drop in temperature and heat transfer rate with reference to slip parameter. Velocity slip together with magnetized hybrid nanofluid flow has been examined by Kakar et al [24]. They observed rise in rate of heat transfer with the rise in melting parameter.

On the basis of above discussion and to venture further in the era of nanofluid flow over wedge, we proposed a mathematical model to represent Falkner-Skan wedge flow with higher order slip in velocity, temperature and concentration incorporating Brownian motion and thermophoresis. Additionally, study includes non-linear thermal radiation. The fluid flow under slip condition differs in great extent from traditional flow.

2. Problem formulation

We consider a steady incompressible magnetized viscous nanofluid flow over a wedge. The free stream velocity is mathematically expressed as power law index of downstream distance x i.e $U_e = U_0 x^m$. U_0 is proportionality constant and as assume to be positive (figure 1). Exponent m is expressed in terms of Hartree pressure gradient parameter$\left(m = \frac{\beta_0}{1-\beta_0}\right)$. Value of m lies between 0 and 1 indicating a wedge flow problem for our investigation. The total angle subtained by two edges of the wedge is $\Omega = \beta_0 \pi$ and half angle between the initial direction of flow and deviated flow on one surface of wedge is $\beta_0 \pi/2$. Flow over a horizontal flat plate corresponds to $m = 0$ $(\beta_0 = 0)$ and stagnation point flow over a vertical plate is represented by m=1 $\left(\beta_0 = \frac{1}{2}\right)$. The surface of the wedge is along x axis and y axis is perpendicular to it. Temperature of surface $T_w$and nanoparticle fraction C_w are considered to be constant. Surface temperature T_w is greater than ambient temperature$(T_w > T_\infty)$, Similarly surface concentration fraction is more than ambient concentration C_∞, $(C_w > C_\infty)$ Non-linear thermal radiation is also considered. The medium over the wedge is considered to be porous. The slip condition is exhibited in a liquid at nanoscale level is nanofluid etc. which is considered in experiments [25,26] describing molecular dynamics and velocity slip at the surface. Similarly, there is a slip condition in temperature and concentration.

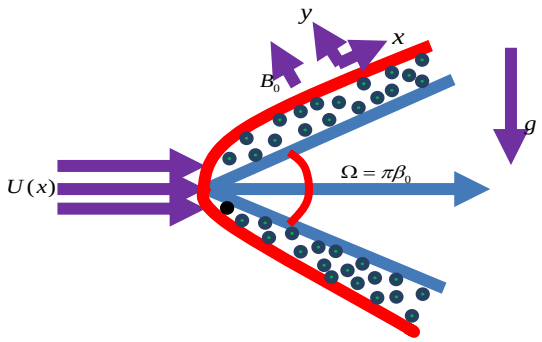

Figure 1. Flow Past a Wedge in Porous Medium with Magnetic Field

Boundary layer equation including Brownian diffusion and thermophoresis can be written as

$$\frac{\partial u}{\partial x} + \frac{\partial v}{\partial y} = 0$$

(1)

$$u\frac{\partial u}{\partial x} + v\frac{\partial u}{\partial y} = U_e\frac{dU_e}{dx} + \nu\frac{\partial^2 u}{\partial y^2} + \frac{\sigma B^2(x)}{\rho}(U_e(x) - u) + g\beta sin\,\Omega/2\,(T - T_\infty) + g\beta^* sin\,\Omega/2\,(C - C_\infty) + \frac{\nu}{k}\,(U_e - u)$$

(2)

$$u\frac{\partial T}{\partial x} + v\frac{\partial T}{\partial y} = \alpha\frac{\partial^2 T}{\partial y^2} + \frac{\nu}{c_p}\left(\frac{\partial u}{\partial y}\right)^2 + \tau\left[D_B\frac{\partial C}{\partial y}\frac{\partial T}{\partial y} + \frac{D_T}{T_\infty}\left(\frac{\partial T}{\partial y}\right)^2\right] - \frac{1}{\rho c_p}\frac{\partial q_r}{\partial y}$$

(3)

$$u\frac{\partial C}{\partial x} + v\frac{\partial C}{\partial y} = D_B\frac{\partial^2 C}{\partial y^2} + \frac{D_T}{T_\infty}\left(\frac{\partial^2 T}{\partial y^2}\right)$$

(4)

With the following boundary conditions

$$u = u_{slip} \quad , \quad v = 0 \quad , \qquad T = T_w + T_{slip} \qquad C = C_{w+}C_{slip} \qquad \text{at} \quad y = 0$$

(5)

$$u = u_e(x) = U_0 x^m \qquad v = 0 \quad , \quad T \to T_\infty \quad , \quad C \to C_\infty \qquad \text{as} \quad y \to \infty$$

(6)

In this context of multiple slip conditions in velocity (1st order and 2nd order)

$$u = u_{slip} = l_1\frac{\partial u}{\partial y} + l_2\frac{\partial^2 u}{\partial y^2}$$

(7)

Here, l_1 and l_2 are 1st order and 2nd order velocity slip parameters respectively. Similarly, 1st order and 2nd order slip conditions in temperature and concentration can be written as

$$T_{slip} = n_1 \frac{\partial T}{\partial y} + n_2 \frac{\partial^2 T}{\partial y^2}$$
(8)

$n_1$and n_2 are 1st order and 2nd order temperature slip parameter respectively.

$$C_{slip} = m_1 \frac{\partial C}{\partial y} + m_2 \frac{\partial^2 C}{\partial y^2}$$
(9)

m_1 and m_2 are 1st and 2nd order concentration slip parameter respectively. Where $\alpha = {k}/{\rho c_p}$ $\left({m^2}/{s}\right)$ is the thermal diffusion parameter, τ is the ratio of specific heat capacity of nanoparticle and base fluid, $\tau = (\rho c)_p/(\rho c)_{bf}$,$c_p$ is the specific heat, ρ is the density of fluid and k is the thermal conductivity. D_B is the Brownian diffusion coefficient and D_T is the thermophoretic diffusion coefficient. q_r is the radiative heat flux. Utilizing the Roseland approximation for optically thick condition $q_r$an be expressed as

$$q_r = -\frac{4\sigma_{SB}}{3k^*}\frac{\partial T^4}{\partial y}$$
(10)

Where σ_{SB} is the Stefan-Boltzmann constant. ($\sigma_{SB} = 5.6647 \times 10^{-8} wm^{-2}k^{-4}$) and k^* is the mean absorption coefficient. Roseland approximation extends the Prandtl number by a factor of thermal radiation. It is to note that due to presence of thermal radiation energy equation is non-linear [27]. So

$$q_r = \frac{-16\sigma_{SB}}{3k^*} T^3 \frac{\partial T}{\partial y}$$
(11)

At the end, the quantities relevant to engineering and technology field are evaluated. The Skin friction coefficient *C f* , local heat transfer coefficient (Nusselt number) *Nux* and local mass transfer coefficient (Sherwood number) *Shx* are defined

$C_f = \frac{(\tau_w)_{y=0}}{\rho U_e^2}$ and $\tau_w = \mu\left(\frac{\partial u}{\partial y}\right)_{y=0}$ is the wall tangential stress.
(12) $Nu_x = \frac{x q_w}{k(T_w - T_\infty)}$ and $q_w = -k\left(\frac{\partial T}{\partial y}\right)_{y=0} + (q_r)_{y=0}$
(13) $Sh_x = \frac{x\, m_w}{D_B(C_w - C_\infty)}$ and $m_w = D_B\left(\frac{\partial C}{\partial y}\right)_{y=0}$
(14)

3. Scheme of Solution

Introducing similarity variable for non-dimensional case,

$$\eta = \left(\frac{U_0 x^{m+1}}{\nu}\right)^{1/2} \frac{y}{x}$$

$$\psi = (\nu U_0 x^{m+1})^{1/2} \qquad F(\eta)$$
(15)

$$\theta(\eta) = \frac{T-T_\infty}{T_w(x)-T_\infty}, \ \phi(\eta) = \frac{C-C_\infty}{C_{w(x)-C\infty}}$$

Temperature and concentration of wall can be expressed as

$$T_w = T_\infty + gx^{2n}$$
$$C_w = C_\infty + hx^{2n} \quad (16)$$

Here, ψ is the stream function, which satisfy the continuity equation (1). Therefore,

$$u = \frac{\partial \psi}{\partial y} \quad \text{and} \quad v = -\frac{\partial \psi}{\partial x} \quad (17)$$

Now substituting equations (11, 15, 16 and 17) in equations (2, 3, 4), we have

$$F''' - [mF' - \left(\frac{m+1}{2}\right)FF'' - m] + (M + k_1)(1 - F') + \lambda_T sin(\Omega/2)\theta + \lambda_M sin(\Omega/2)\phi = 0 \quad (18)$$

$$2nF'\theta - \left(\frac{m+1}{2}\right)F\theta' = \frac{\theta''}{Pr} + Ec(F'')^2 + N_b\theta'\phi' + N_t(\theta')^2 + \frac{1}{Pr}\frac{4}{3}N_R[\{1+\theta(\theta_w-1)\}^3\theta']' \quad (19)$$

$$\phi'' + \theta''\frac{N_t}{N_b} = LePr\left(2nF'\phi - \frac{m+1}{2}F\phi'\right) \quad (20)$$

Prime denotes differentiation with respect to η. The non-dimensional quantities are

$M = \frac{\sigma B_0^2}{\rho U_0}$ (Magnetic parameter)

$k_1 = \frac{\nu x^{1-m}}{kU_0}$ (Permeability parameter)

$\lambda_T = \frac{g\beta x(T_W(x)-T_\infty)}{{U_0}^2 x^{2m}} = \frac{Gr_x}{Re_x^2}$ (Thermal convective parameter)

The ratio of buoyancy force to inertia force is represented by λ_T. This parameter is also called as mixed convection parameter. Free convection region is represented by $\lambda_T >> 1$. Forced convection regions denoted by $\lambda_T << 1$. Free and forced convection region are of comparable magnitude when $\lambda_T = 1$.

$\lambda_M = \frac{g\beta^* x(C_w(x)-C_\infty)}{U_0^2 x^{2m}} = \frac{Gm_x}{Rex^2}$ (Mass convective parameter)

$Pr = \frac{\nu}{\alpha}$ (Prandtl number

$D_B = \frac{K_B T}{3\pi\mu d_p}$ (Brownian diffusion coefficient)

Where K_B the Boltzmann is constant, μ is the nanofluid viscosity, d_p is the particle diameter.

$D_T = \frac{\bar{\beta}\,\mu C}{\rho}$ (Thermal diffusion coefficient)

$\bar{\beta} = 0.26k_f/(2k_f + k_p)$ is the thermophoretic coefficient. k_f and k_p denote the thermal conductivity of the fluid and nanoparticle respectively.

$N_b = \frac{\tau D_B h x^{2m}}{\nu}$ (Brownian diffusion parameter)

$N_t = \frac{\tau D_T h x^{2n}}{\nu T_\infty}$ (Thermophoretic parameter)

$N_R = 1/\frac{kk^*}{4\sigma^* T_\infty^3}$ (Radiation parameter)

$\mathrm{Ec} = \frac{U^2}{C_P(T_{w(x)-T_\infty})}$ (Eckert number)

$\theta_w = \frac{T_w}{T_\infty}$ (>1) (Temperature ratio parameter)

$Le = \frac{\alpha}{D_B}$ (Lewis number)

.

In view of transformations (5), (6), (7), (8) and (9) new boundary conditions are

$F'(0) = \alpha_1 F''(0) + \alpha_2 F'''(0)$

(21)

$F(0) = 0$ at $\eta = 0$

(22)

Where

$\alpha_1 = p_1 \left(\frac{U_0}{\nu}\right)^{1/2} x^{\frac{m-1}{2}}$ (1st order velocity slip parameter)

$\alpha_2 = p_2 \frac{U_0}{\nu} x^{m-1}$ (2nd order velocity slip parameter)

$\theta(0) = 1 + \gamma_1 \theta'(0) + \gamma_2 \theta''(0)$ at $\eta = 0$ (23)

Where

$\gamma_1 = n_1 \left(\frac{U_0}{\nu}\right)^{1/2} x^{\frac{m-1}{2}}$ (1st order temperature slip parameter)

$\gamma_2 = n_2 \left(\frac{U_0}{\nu}\right) x^{m-1}$ (2nd order temperature slip parameter)

$\phi(0) = 1 + \delta_1 \phi'(0) + \delta_2 \phi''(0)$ at $\eta = 0$

(24)

Where

$\delta_1 = m_1 \left(\frac{U_0}{\nu}\right)^{1/2} x^{\frac{m-1}{2}}$ (1st order concentration slip parameter)

$\delta_2 = m_2 \left(\frac{U_0}{\nu}\right) x^{m-1}$ (2nd order concentration slip parameter)

and

$F'(\infty) = 1$, $\theta(\infty) = 0$, $\phi(\infty) = 0$

(25)

At last the dimensionless skin friction coefficient, local heat transfer coefficient and mass transfer coefficient are derived from equations (12), (13) and (14) respectively.

$$C_f {Re_x}^{1/2} = F''(0) \quad (26)$$

$$Nu_x {Re_x}^{-1/2} = -\theta'(0)\left[1 + \frac{4N_R}{3}\{1 + (\theta_w - 1)\theta(0)\}^3\right] \quad (27)$$

$$Sh_x = -\phi'(0){Re_x}^{1/2} \quad (28)$$

4. Results and Discussion

The boundary value problem relating to nonlinear ordinary differential equation has been solved by employing fourth order Runge-Kutta method in association with shooting technique. The source of error may rise due to infinite boundary condition. In order to make numerical domain finite, we considered computational domain to be sufficiently large. The grid size is considered as 0.01 to achieve accuracy of the order of 10^{-5}.The value of different parameters used are taken as $M = 1,\ m = 0.01,\ \lambda_T = \lambda_M = 0.01,\ Nt = 0.3, Nb = Nr = Ec = 0.5,$ $K_1 = 0.5,\quad \Pr = 1,\quad \theta_w = 1.2,\quad Le = 1,\quad \beta = 0.5,\quad \alpha_1 = \alpha_2 = 0.01,$, $\gamma_1 = \gamma_2 = 0.1, \delta_1 = \delta_2 = 0.01, n = 0.5$.

4.1 Validation

In order to obtain accuracy of numerical results achieved in this analysis, first of all we verified our results under simplified assumption with previously published papers. We have calculated skin friction coefficient and compared the results with Ariel [28], Srnivasacharya et al. [29] and Mishra et al. [15] and conclude that results are in excellent agreement as shown in table1.

Table 1. Skin Friction Coefficient F" (0) for Several Values of Magnetic Parameter M

M	Ariel [28]	Srinivasacharya et al [29]	Mishra et al [15]	Present
0	1.232588	1.232587	1.232587	1.232645
1	1.585331	1.585330	1.58533	1.585110
4	2.34663	2.346869	2.346661	2.346700
25	5.147965	5.147964	5.147959	5.147865
100	10.074741	10.074741	10.974733	10.074770

4.2 Velocity Characteristics of Nanofluid over wedge

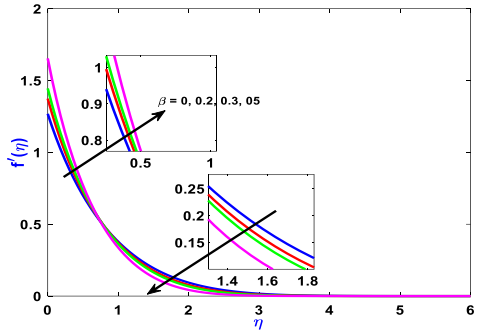

Figure 2. Velocity Profiles for Several Values of β_0

Dimensionless velocity profiles for several values of β_0 are shown in figure 2. This plot signifies two kinds of wedge flow namely (i) flow over a flat plate (β_0=0) and stagnation flow (β_0=1). Physically this shows, how boundary layer behaves to pressure gradient. Flow pattern indicates increase in velocity from flow over flat plate to flow over wedge. However, flow reversal occurs at $\eta \approx 0.8$.

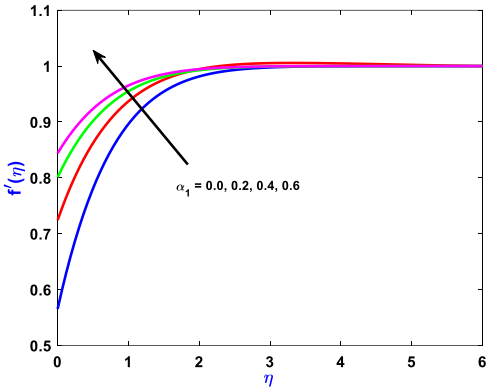

Figure 3. Dependence of Velocity Parameter for Several Values of α_1

Variation of fluid velocity for several values of 1st order slip parameter are depicted in figure 3. Sharp increase in velocity is observed with rise in1st order slip parameter corresponding to non-dimensional parameter in the range $0 \leq \eta \geq 3$.Thicknes of velocity field falls in enhancing 1st order slip parameter. Away from the surface i.e., $\eta \geq 3$ slip effects disappears and velocity become constant. Physically the velocity gradient at the wall is maximum and minimum at the free stream. This implies velocity gradient is not linear across boundary layer. In this context increasing 1st order slip parameter the velocity of flow increases.

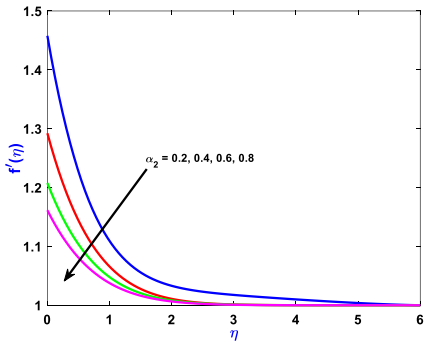

Figure 4. Dependence of Velocity Parameter for Several Values of α_2

We have studied the effect of second order slip parameter on velocity profiles (figure 4). Liquid molecules strike the surface in all direction. The net momentum transfer on the wall is contributed by molecules striking the surface and molecules reflected back from the surface. This is the contribution of second order slip parameter therefore velocity drops due to rise in second order slip parameter.

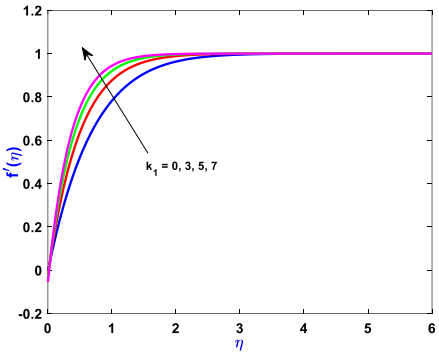

Figure 5. Dependence of Velocity Parameter for Several Values of K_1

Impact of permeability parameter is reflected in figure.5. Permeability increases means porosity reduces causing velocity of flow to raise. This is interpreted with the fact that thickness of velocity field decreases. Away from the surface $\eta \geq 3$ velocities are independent of permeability parameter.

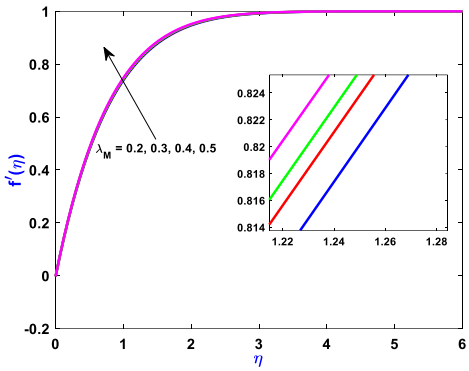

Figure 6. Dependence of Velocity Parameter on Several Values of λ_M

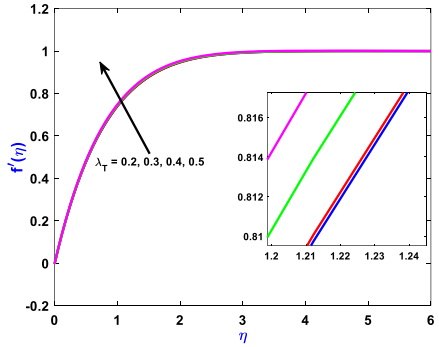

Figure 7. Dependence of Velocity Parameter for Several Values of λ_T

Figure 6 and 7 represents effects of mass convective parameter and thermal convective parameter on velocity profiles. Rise in thermal convective parameter or mass convective parameter implies temperature or concentration is more near the wall. That effectively

enhances the temperature or concentration on the wall. Subsequently temperature field or concentration field thickness reduces.

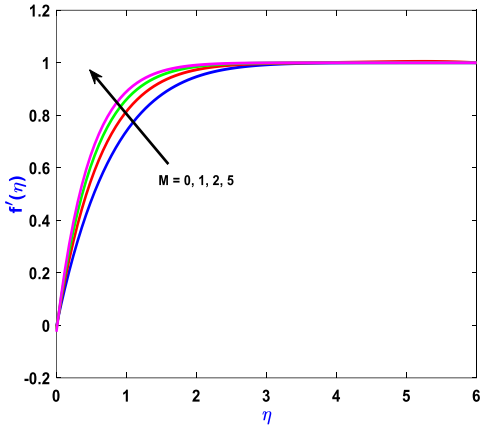

Figure 8. Dependence of Velocity Parameter on Several Values of M

Magnetic field (figure 8) has significant effect on velocity field. Velocity profiles for different values of M are shown above. In the absence of magnetic field (M=0) viscosity dominates the flow and velocity reduces. For large values of M viscosity significantly falls causing velocity of fluid flow increases.

4.3 Temperature Characteristics of Nanofluid Flow

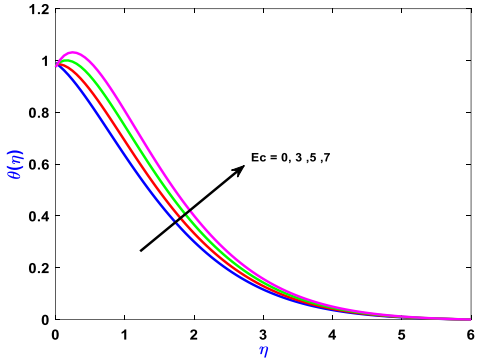

Figure 9. Temperature Profiles for Different Values of Eckert Number *Ec*

Viscous dissipation parameter (Ec) signifies conversion of kinetic energy into potential energy by virtue of doing work against stress of viscous fluid. Large values of Ec signifies rise in temperature due to frictional force. For higher values of Ec inflection point tries to occur near the surface and falls rapidly to zero value away from the surface (figure 9).

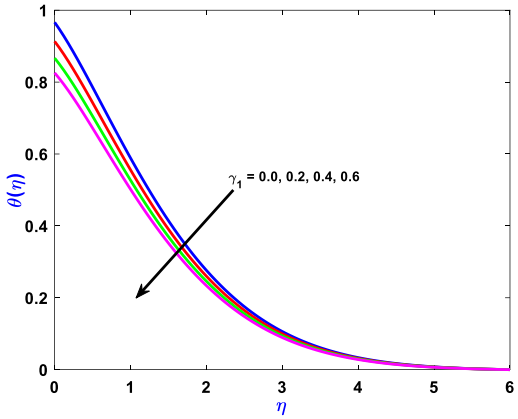

Figure 10. Temperature Profiles for Several Values of 1st Order Temperature Slip Parameter γ_1

For continuum flow (high density) temperature of surface is assumed to be wall temperature. But in case of low-density molecular flow and wall temperature is different from surface temperature causing temperature gradient to exist. For higher values of 1st order slip parameter temperature gradient is less. Temperature decreases slowly to zero value (figure 10).

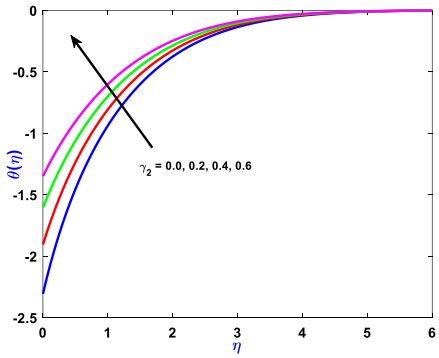

Figure 11. Effect of 2nd Order Slip Parameter on Temperature γ_2

This effect is quite interesting. Temperature reversal occur causing wall temperature to be less than ambient. Therefore heat flows from surface to wall (cold wall conditions). Higher values of parameter mean temperature falls slowly compared to large value of 2nd order slip parameter (figure 11).

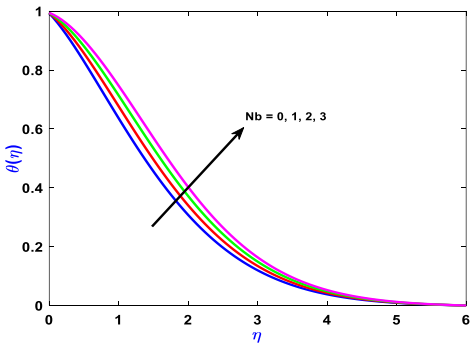

Figure 12. Temperature Profiles vs. N_b

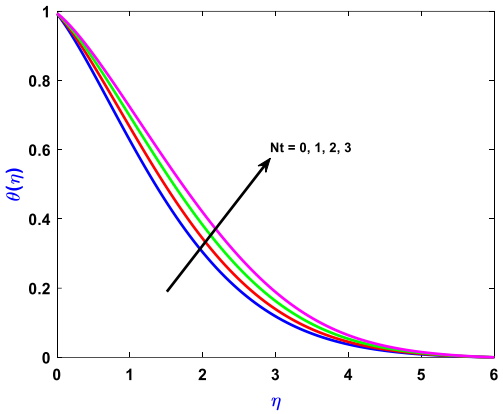

Figure 13. Temperature Profiles vs N_t

Figures 12 and 13 describe dependence of temperature on Diffusion parameter N_b and N_t Thermophoresis parameter Nt. In both cases temperature starts from unity value at the surface and decreases to zero value away from the surface. However, temperature gradient is more for small values of N_b and N_t than for large values of N_b and N_t respectively.

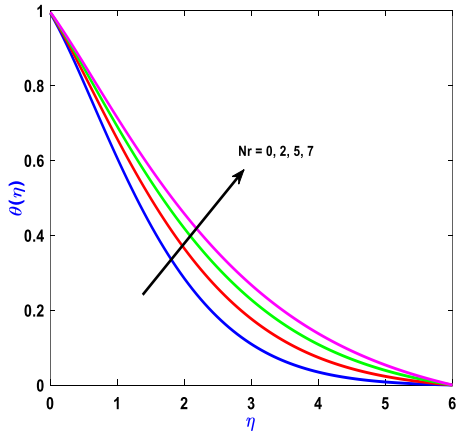

Figure 14. Variation of Temperature with Thermal Radiation Nr

Figure 14 deals with variation of temperature with thermal radiation parameter. Heat transfer is contributed by (i) Heat transfer due convection and (ii) Heat transfer due to radiation. More and more heat is transported from surface to fluid causing an increase in temperature of fluid. These variations are shown above.

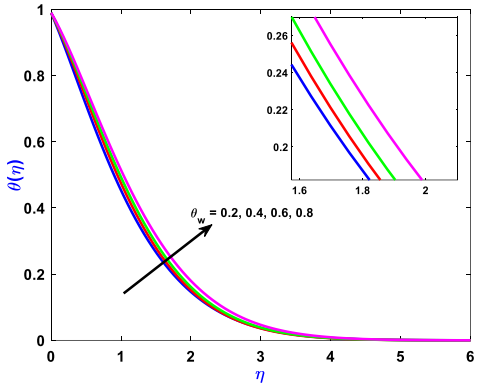

Figure 15. Variation of Temperature Profiles for Different Values of Temperature Ratio Parameter θ_w

Temperature profiles for different values of temperature ratio parameter are depicted in figure 15. This effect are due to the extra source in the boundary layer. Because of this additional term in energy equation, more heat is transferred to fluid causing an increase in temperature of fluid.

4.4 Concentration Characteristics of Nanofluid Flow

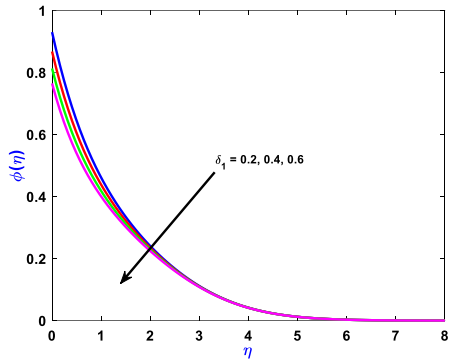

Figure 16. Concentration Characteristics for Different Values of 1st Order Slip Parameter δ_1

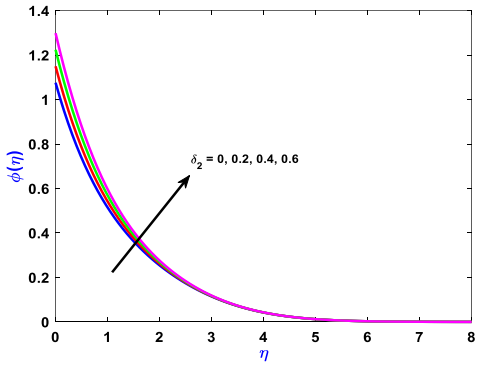

Figure 17. Concentration Characteristics for Different Values of 2nd Order Slip Parameter δ_2

Volume fraction profiles for several values of 1st order slip parameter and 2nd order slip parameter are depicted in figures 16 and 17 respectively. Near the molecular density is large. Therefore, more molecules strikes the surface. This leads to enhancement in volume fraction. However away from the surface molecular density falls. This tends to decrease in volume fraction away from the surface. Slip effects is prominent near the wall. Beyond $\eta \geq 3$ slip effects diminishes.

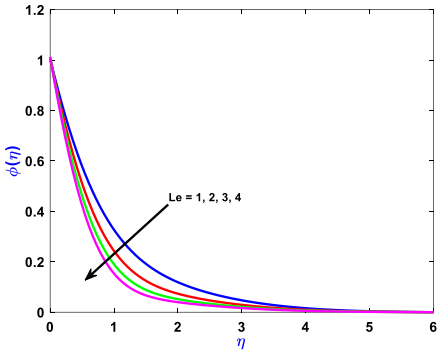

Figure 18. Volume Fraction Variations with respect to Lewis Number *Le*

Lewis number established a relation between mass transport to heat transport in presence of heat and mass transfer in case of fluid. Larger Le indicates mass transport being more than heat transport. Therefore, more mass being transfer from surface to fluid. Hence volume fraction near the surface drops sharply as indicated in figure 18. However, in all cases volume fraction attains maximum value at the wall and gradually reduces to zero away from the surface.

Skin friction coefficient is shown in Table 2 for different values of physical parameters. Magnetic field causes induction drag and this drag is small when M is small. In that case skin friction is contributed by viscous drag alone. But the application of magnetic field in presence of viscous drag enhances the skin friction further. Increase in 1st order slip brings about decrease in skin friction and 2nd order slip parameter brings about increase in skin friction. in Besides permeability parameter, thermal convective parameter and mass convective parameter increase the skin friction coefficient.

Table 2. Calculation of Skin Friction Coefficients for Various Values of Physical Parameters

M	α_1	α_2	K_1	λ_T	λ_M	$C_f Re_x{}^{1/2}$
1						1.2728
2						1.6302
3						1.9308
4						1.6289
1	0.01					1.654
	0.02					1.6289
	0.03					1.6044
	0.04					1.5806
	0.01	0.01				1.654
		0.02				1.694
		0.03				1.736
		0.04				1.7801
		0.01	3			2.0678
			4			2.3237
			5			2.5616
			6			2.7864

			3	2		1.8171
				3		2.0829
				4		1.6616
				5		2.6056
				2	1	1.2953
					2	1.37
					3	1.4321
					4	1.7564

Local heat transfer coefficient is tabulated for various values of physical parameter (table 3). Increasing Prandtl number implies reduction in thermal diffusivity, which cause fall in heat transfer coefficient. Thermal radiation adds to thermal diffusion initially present in the model. This extra term causes increase in heat transfer coefficient. Viscous dissipation causes temperature of wall to rise. This resulted in higher differential temperature and ultimately higher heat transfer coefficient. It is interesting to discuss effects of 1st order and 2nd order slip parameter on Nusselt number. It is noteworthy to mention that slip effect is contributed by molecular diffusion. Heat is carried by molecules and transfer it to the wall when it strikes the wall. Therefore, reduction in heat transfer coefficient is observed.

Table 3. Calculation of Heat transfer coefficient for various values of physical parameters.

Pr	Nr	Ec	γ_1	γ_2	$Nu_x Re_x^{-1/2}$
1	2	5	0.4	0.7	-0.6597
2					-0.5965
3					-0.4607
4					-0.3064
1	2				-1.3835
	4				-2.1455
	6				-2.8325
	8				-3.4882
	2	1			-0.4209
		3			0.5433
		5			1.52
		7			2.5061
		1	0.2		-0.566
			0.4		-0.4901
			0.6		-0.4309
			0.8		-0.3838
			0.4	0.1	-0.5925
				0.3	-0.4685
				0.5	-0.3717
				0.7	-0.2858

Lewis number ordinarily concern with mass transfer and heat transfer. Higher Lewis number increases mass transfer ratio. Brownian diffusion parameter as well thermophoretic parameter diminishes local Sherwood number. It is pertinent to mention the effect of slip parameter. Ist order slip parameter alone reduces mass transfer coefficient, while 2nd order slip parameter together with 1st order slip parameter raise the Nusselt's number.

Table 4. Calculation of Mass Transfer Coefficient for Various Values of Physical Parameters.

Le	N_b	N_t	δ_1	δ_2	$Sh_x Re_x^{-1/2}$
1	0.4				-0.7761
2					-1.0422
3					-1.353
4					1.2174
1	0.2				-1.353
	0.4				-0.7796
	0.6				-0.7741
	0.8				-0.7718
	0.4	0.1			-0.7702
		0.4			-0.7638
		0.2			-0.7537
		0.3			-0.7404
		0.3	0.1		-0.7285
			0.2		-0.6771
			0.3		-0.6345
			0.4		-0.5969
			0.1	0.2	-0.8832
				0.4	-0.9975
				0.6	-1.1134
				0.8	-1.2308

5. Conclusions

Heat and mass transfer analysis of nanofluid has been analysed considering Brownian motion and thermophoresis together with non-linear thermal radiation. Since the fluid under discussion is in nanoscale level, it is essential to consider higher order slip effects. Flow behaviour in relation to different physical parameters are calculated numerically and depicted graphically. The results obtained are outlined here.

(i) Behaviour of boundary layer with respect to pressure gradient are depicted. It is observed that velocity of wedge flow increases with respect to wedge angle.

(ii) When M=0, velocity alone controls the flow. For large value of M, both induction drag and viscous drag control the flow. Because of additional drag skin friction coefficient decreases.

(iii) For a medium with large porosity, permeability to the flow decreases and that result in decrease in velocity.

(iv) Slip effects in velocity are important particularly flow in nanoscale level. According to kinetic theory net momentum transfer depends on molecules striking the wall and molecules diffusively reflected back.1st order slip increases velocity and 2nd order decreases velocity.

(v) For 1st order slip (large γ_1) temperature gradient is small, therefore less heat is being transported to fluid raising surface temperature. However, temperature gradient is more in case of second order slip causing temperature of surface to fall.

(vi) In case high density molecular flow temperature of wall is same as that of surface.
But in case low density flow there exist a temperature gradient between the surface and wall.

(vii) Effects of Brownian diffusion parameter and thermophoresis parameter are significant near the surface and reduce gradually to zero value away from the surface.

(viii) Effect of second order slip parameter with 1st order slip parameter is more than the 1st order slip parameter alone. Slip parameter effects are significant near the wall and reduces to zero away from the surface.

(ix) Large Lewis number indicate sharp fall in volume fraction compared to small Lewis number.

Acknowledgement

We sincerely thank Professor S R Mishra of SOA University, Bhubaneswar, for his valuable suggestion in improving this work.

References

*[1] Choi S.U. S, Zhang W.Yu. Lockwood, F.E, Grulke E.A, "Anomalous thermal conductivity enhancement in nanotube suspensions", Appl.Phys.**(2001)**,79, pp 2252-2254.*

*[2] Akoh H, Tsukaasaki Y, Yatsuya S, Tasaki, "A Magnetic properties of ferromagnetic ultrafine particles prepared by a vacuum evaporation on running oil substrate", Cryst Growth, **(1978)**, 45, pp495-500.*

*[3] Eastman J. A, Choi S.U.S, Li S, Thomson L J, lee S," Enhanced thermal conductivity through the development of nanofluid Materials research society symposium proceedings", Material research society, Pittsburgh, PA, USA, Boston, MA, USA, **(1977)**,457, pp 3-11.*

*[4] Yu W, Xie H, "A review on nanofluids; Preparation, Stability Mechanism and Applications", Journal of Nanofluids, **(2012)**, 2012, ID 435873.*

*[5] Buongiorno J, "Convective transport in nanofluids", J Heat transfer, **(2006)**, 128(3), pp 240-250.*

*[6] Tiwari R.K, Das M. K, Heat transfer augmentation in a two-sided lid driven differentially heated square cavity utilizing nanofluids, Int J Heat Mass Transfer, **(2017)**, 50, pp2002-2018.*

*[7] Liang G and Mudawar I, "Review of single phase and two phase nanofluid heat transfer in macro-channels and micro-channels", Int.J. Heat Mass Transfer, **(2019)**,136.324-354.*

*[8] Yildiz O, Acikgoz O, Yilidz G, Bayrak M, Dalkilic A.S, Wongwises, "Single phase flow of Nanofluid including graphite and water in a microchannel", Heat and Mass Transfer, **(2020)**, 56, pp1-24.*

*[9] Jamshed W, Nisar K. S, Isa Mohamed S.S.P, Batool S, Abdel-Aty Abdeli H, Zakarya M, "Computational case studies in tangent hyperbolic hybrid nanofluid flow single phase thermal investigation", Case studies in Thermal Engg., **(2021)** ,27,101246.*

[10] Jamshed W, Nisar K.S, Gowda R. J. Punith, Kumar R. N, Prasannakumar B. C, Radiative heat transfer on second grade nanofluid flow past a porous flat surface: a single-phase mathematical model", Physica Scripta, ***(2021)****,96(6), Id-96064006.*

[11] Sheikholeslami M, "Cuo-Water nanofluid flow due to magnetic field inside a porous media considering Brownian motion", Journal of Molecular liquids, ***(2018)****,249, pp 921-929.*

[12] Sheikholeslami M, Ganji D.D, "Nanofluid convective heat transfer using semi analytical and numerical approaches, A review". Taiwan Inst. Chem. Eng. ***(2016)*** *65, pp 43-77.*

[13] Sheikholeslami M, Ganji D D, Javed M. Y, Ellahi R, "Effect of thermal radiation on Magneto hydrodynamics nanofluid flow and heat transfer by means of two-phase model", Journal of Magnetism and Magnetic materials, ***(2015)****, 374(15), pp 36-43.*

[14] Ali M, Alim M. A, Nasrin R, Alam M. S, Munshi M J H, "Similarity solution of unsteady MHD boundary layer flow and Heat transfer past a moving wedge in a nanofluid using the Buongiorno Model", Procedia Engineering, ***(2017),*** *194, pp 407-413.*

[15] Mishra P, Acharya M R, Panda S, "Mixed convection MHD nanofluid flow over a wedge with temperature dependent het source", Pramana-J. Physics, ***(2021)****, 95, ID 95:0052.*

[16] Acharya M Mishra P, Panda, "Thermodynamic optimization of nanofluid flow over a non-isothermal wedge with non-linear radiation and activation energy", Physica Scripta, ***(2022)****, 97(1), ID-97015204.*

[17] Wu Lin, "A slip model for rarefied gas flows at arbitrary Knudsen number", Applied physics letters, ***(2008)*** *,93, pp 253103.*

[18] Martin M J, Boyd I D, "Falkner-Skan flow over a wedge with slip boundary condition", Journal of thermophysics and heat transfer, ***(2010)****, 24(2), pp 263-270.*

[19] Awais M, Hayat T, Ali A, Irum "Velocity, thermal and concentration slip effects on a magneto-hydrodynamic nanofluid flow", Alexandria Engineering Journal, ***(2016)****, 55, 2107-2114.*

[20] Liu Q, Zhu J, Bin-Mohsin, Zheng, "Hydromagnetic flow and heat transfer with a various nanoparticles additive past a wedge with high order velocity slip and temperature jump", Canadian Journal of Physics, ***(2017)****, 95(5), pp440-449.*

[21] Pandey A K and Kumar M, Effect of viscous dissipation and suction/injection on MHD nanofluid flow over a wedge with porous medium and slip, Alexandria Engineering Journal, (2016), 55, pp3115-3123.

[22] Khan M, Azam S, Alshammari, "Unsteady slip flow of Carreau nanofluid over a wedge with nonlinear radiation and new mass flux condition", Results in Physics, ***(2017)****, 7, pp 2261-2270.*

[23] Ramya D, Srnivas Raju R, Anand Rao, Chamkha, "A Effects of velocity and thermal wall slip on magnetohydrodynamics (MHD) boundary layer viscous flow and heat transfer of a nanofluid over a non-linearly stretching sheet: a numerical study", Propulsion and Power research, ***(2018)****, 7(2), pp 182-195.*

[24] Kakar N, Khalid A, Al-Johani A S, Alshammari N, "Melting heat transfer of a magnetized water-based hybrid nanofluid flow past over a stretching /shrinking wedge", Case Studies in Thermal Engineering, ***(2022)****, 30, pp 101674.*

[25] Watanable W, Yanuar Mizunama, "Slip of Newtonian fluids at solid boundary", JSME Internatinal Journal, Ser B, ***(1998)****, 41(3), pp 525-529.*

*[26] Tretheway D C. Meinhart C D, "Apparent fluid slip at hydrophobic microchannel walls, Physics of fluids", **(2002)**,14(3), pp L9-L12.*
*[27] Smith W Effect of gas radiation in boundary layer on aerodynamic heat transfer, J Aerosol Science, **(1952)**, 20, pp 579-580.*
*[28] Ariel P D, "Hiemenz flowin hydromagnetics", Acta Mechanica, **(1994)**,103, pp31-43.*
*[29] Srnivasacharya D, Mendu U, Venumadhva K, "MHD boundary layer flow of a Nanofluid past a wedge", Procedia Engineering, **(2015)**,127, pp. 1064-1070.*